Elastic scattering of positive pions on ^{16}O at 40.0 and 49.7 MeV

D. J. Malbrough, C. W. Darden, R. D. Edge, T. Marks, and B. M. Preedom
University of South Carolina, Columbia, South Carolina 29208*

R. L. Burman, M. A. Moinester,† and R. P. Redwine
Los Alamos Scientific Laboratory,‡ Los Alamos, New Mexico 87545

F. E. Bertrand, T. P. Cleary, E. E. Gross, and C. A. Ludemann
Oak Ridge National Laboratory,§ Oak Ridge, Tennessee 37830

K. Gotow
Virginia Polytechnic Institute and State University,¶ Blacksburg, Virginia 24061
(Received 15 September 1977)

Differential cross sections for elastic scattering of positive pions on ^{16}O at 40.0 and 49.7 MeV were measured at about 10° intervals for laboratory angles from 25° to 160°. Relative uncertainties between angles are 3%, with the overall normalization known to 7% for each angular distribution. The angular distributions are similar in shape, being dominated by a minimum at about 60°. The differential cross sections are presented along with the results of a partial wave analysis which gives good fits at both 40.0 and 49.7 MeV. The data are also fitted by a simple phenomenological first-order Kisslinger nonlocal optical model calculation.

[NUCLEAR REACTIONS $^{16}O(\pi^+,\pi^+)^{16}O$. $E=40.0$, 49.7 MeV, $\theta=25$–160°, measured $\sigma(\theta,E)$. Partial-wave and optical model analyses of $\sigma(\theta,E)$.]

I. INTRODUCTION

For several years now, high quality pion-nucleus elastic scattering data[1] have existed for energies in the region of the (3, 3) resonance. These data have been well reproduced by simple first-order optical model calculations.[2-5] The success of the simple optical model potentials, and the lack of sensitivity of the angular distributions to the theoretical parameters and assumptions used, is probably a result of the large absorption of the pion at these energies. Thus elastic scattering at (3, 3) resonance energies is not likely to provide much new information about pion-nucleus interactions. In contrast, low-energy scattering should be sensitive to higher-order effects in the optical model calculation.[6-10] The need for high quality pion-nucleus elastic scattering data at energies below 75 MeV is clear. As part of such an experimental survey[11] we present results for π^+ elastic scattering on ^{16}O at 40.0 and 49.7 MeV.

II. EXPERIMENTAL TECHNIQUES AND APPARATUS

The experiment was carried out on the low-energy pion channel[12] at the Clinton P. Anderson Meson Physics Facility of the Los Alamos Scientific Laboratory. A positive pion beam with an average pion flux of about 3×10^6 per second and a momentum acceptance $\Delta p/p=1\%$ was used. The beam spot on a 7.5 cm^2 water target was 20 mm full width at half maximum (FWHM) horizontally and 8 mm FWHM vertically as measured with a multiwire profile monitor.[13] The beam divergence distribution had a σ of approximately 66 mrad horizontally and 24 mrad vertically (in the scattering plane). The water was gelled with a 1.5% gelatin mixture and sandwiched between two 12.7 μm plastic sheets fastened on an aluminum target frame which was mounted at 45° to the pion beam direction. An identical target frame, with no water, was used for target-out background measurements. The target thickness was 390 mg/cm^2. The pion energies at the center of the target were $T_\pi=49.7$ and $T_\pi=40.0$ MeV.

Plastic scintillator detector telescopes in a multidetector array were used for the measurements. These detectors are described in more detail elsewhere.[14] The detector telescopes consisted of two scintillator elements: a 3 mm thick, 1.9 cm diam ΔE scintillator mounted in front of a 12.7 cm thick E scintillator in which the scattered pions stopped. Ten telescopes were distributed in reflection and transmission geometries to view scattering in the vertical plane. The typical target-detector distance was 25.4 cm giving a geometric solid angle of about 4.35 msr. Two angle sets were used to take measurements from 25° to 160° at a total of 18 different angles. A typical run lasted six hours per angle set. Two detectors, one in transmission geometry and one in reflection geometry, remained fixed to check the internal normalization between the angle sets.

Because 10 angles were measured simultaneously with identical detectors, we are confident that the relative differential cross sections were determined to the 2–3% accuracy quoted. The beam was monitored during the data runs with two 2.5 cm thick scintillators placed on opposite sides of the target in the horizontal plane (one at 90°) to detect particles in coincidence. The spectrum in the 90° monitor consisted mostly of protons from $(\pi^+, 2p)$ reactions and was calibrated at a pion rate of about 10^5/sec with a monitor placed in the beam. The in-beam monitor incorporated two 1.9 cm thick plastic scintillators whose two-dimensional spectrum provided good pulse-height separation between π's, μ's, and e's. Using this method of normalization the values (good to about 10%) we obtain for π^+-p differential cross sections are consistent with the data of Bertin *et al.*[15]

The requirement for processing an event from a telescope was generally only an E-ΔE coincidence. The analog-to-digital converter gate was set to integrate the signal for 110 nsec, during which time about 95% of the stopped pions decayed to muons without the muons in turn decaying to positrons. The remaining 5% of the elastically scattered pions which did not satisfy this condition fell outside the elastic peak. Muons from the decay of pions in the beam subjected the two most forward-angle detectors to a high background that could not be discriminated against by just an E-ΔE coincidence requirement. Therefore, an additional logic requirement was placed on these systems which demanded the 4.1 MeV muon signal from the decay of the stopped pion follow the E-ΔE coincidence. These "π-μ" systems, similar to those described by Axen *et al.*,[16] operated at about 50% efficiency for detecting π's. The efficiency was set primarily by the magnitude of the dead time ($\simeq$20 ns) between a pion stop and initiation of a gate ($\simeq$100 ns long) for detecting a subsequent $\pi \rightarrow \mu$ decay. The efficiencies of the π-μ systems were determined by comparing measurements of elastically scattered π^+'s at 140° with the π-μ and with the "E-ΔE" logic requirements. The uncertainty in these efficiency determinations was typically 3%. Measurements of electronics dead time during data runs were made with a pulser system and found to be less than 0.5%.

Data were recorded event by event using a data acquisition system[17] with a PDP 11/45 computer. Two-dimensional E-ΔE plots from the telescopes were obtained. Following cuts on the ΔE spectrum and the target-out-background subtraction, typical projected energy spectra in the E detector are shown in Fig. 1 for two angles. The elastic peaks

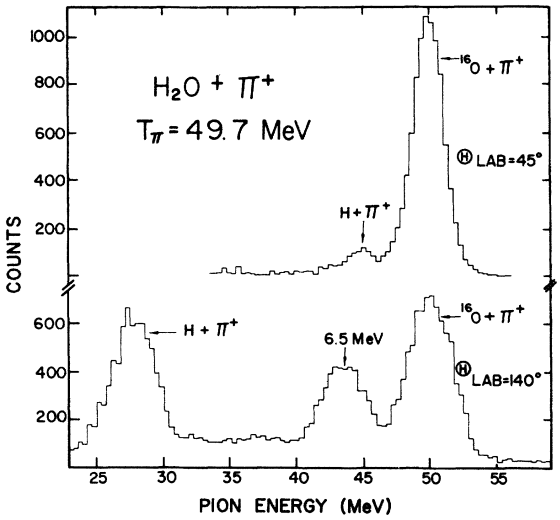

FIG. 1. Energy spectra of 49.7 MeV positive pions scattered at 45° and 140° on an H_2O target.

from π^+ scattering on ^{16}O and on the protons in the water target, as well as an envelope of peaks for the 140° spectrum at an ^{16}O excitation of about 6.1 MeV, are clearly seen. Statistical uncertainties in the number of counts in the π^+-^{16}O elastic peaks were typically less than 2%. The energy resolution was determined primarily by target thickness and ranged from 4 MeV FWHM for the worst case in reflection to about 2 MeV FWHM for the best case in transmission. The intrinsic resolution of the detectors at 50 MeV was measured in calibration runs, using the direct beam, to be about 1.3 MeV FWHM.

Various corrections to the data were required. A subtraction for scattering from protons in the water target at angles below 50° was made since the resolution was not sufficient to separate the π's scattered from protons and from ^{16}O. The subtraction was based on a phase shift calculation[18] which agrees well with recent π^+-p elastic scattering data.[15] The subtraction was never more than a 3% correction to the cross section. Systematic corrections which were common to all detectors or which were necessary for the normalization procedure are listed, with their uncertainties, in Table I.

We have also considered corrections for the finite geometry of the beam, for the finite 4° acceptance of the detectors, and for multiple scattering in the target. These corrections, which are necessary to compare experiment and theory in an angular region where $d\sigma/d\Omega$ is changing rapidly and nonlinearly, were carried out according to the prescription given by Friar and Negele[19] using the experimental parameters given above. A partial-wave fit (described in Sec. IV) to the

TABLE I. Important corrections to the data which affect the overall normalization.

Correction	Size of correction 40.0 MeV	49.7 MeV
Pion decay [a]	(1.9 ± 0.5)%	(1.6 ± 0.5)%
Pion-nuclear reactions [b]	(1.6 ± 0.4)%	(2.0 ± 0.5)%
Pion elastic scattering [c]	(0.5 ± 0.4)%	(0.9 ± 0.5)%
Systematic errors [d]	4.0%	4.0%

[a] This correction includes the effects of pion decay between target and telescopes, while stopping in telescopes and between target and in-beam monitor counters during calibration runs. Because the target-to-telescope and the target-to-monitor counters distances are similar, there is considerable cancellation of decay corrections.

[b] This correction includes estimates for pion reactions in the target, in the detector telescopes, and in the in-beam monitor counters during calibration runs. As with the case of the decay estimates, there is cancellation of corrections to give a fairly small correction to the overall normalization. The uncertainties are primarily due to uncertainties in the estimates of reaction cross sections.

[c] Like the other two corrections, the elastic scattering correction to the overall normalization involves some cancellation of corrections to the detector telescope data and the monitor calibration data.

[d] This error is determined by the reproducibility of the absolute cross sections from separately normalized runs.

uncorrected data was used as a first approximation to the true shape of the angular distribution. An iterative procedure of correcting the data and then refitting was used to obtain the final corrections for effects of finite solid angle, finite beam geometry, and multiple scattering. Because the corrections were small (9% at the most sensitive angle) one iteration was sufficient.

III. EXPERIMENTAL RESULTS

The 40.0 and 49.7 MeV differential cross sections are listed in Table II. The data in the fourth column of Table II have been corrected for effects of finite solid angle, finite beam geometry, and multiple scattering, as described in Sec. II. The measured differential cross sections (column 4 of Table II) are plotted in Figs. 2 and 3. The error bars indicate only relative uncertainties from point to point. In addition there is a normalization uncertainty of 7% for each angular distribution.

The angular distributions are seen to be quite similar in shape; both are dominated by a minimum at about 60°. This structure is similar to that observed in 50 MeV π^+ scattering on ^{12}C.[8,10] The minimum can be interpreted as being due to interference between the s- and p-wave pion-nucleon amplitudes. The most obvious difference between the 40.0 and 49.7 MeV distributions is the faster falloff at back angles seen in the 49.7 MeV data.

TABLE II. Differential cross sections for π^+-^{16}O elastic scattering at T_π=40.0 MeV and T_π=49.7 MeV.

$T_{\pi_{lab}}$ (MeV)	$\theta_{c.m.}$ (deg)	$\frac{d\sigma}{d\Omega_{c.m.}}$ (mb/sr) [a]	$\frac{d\sigma}{d\Omega_{c.m.}}$ (mb/sr) [b]
40.0	25.3	20.96 ± 2.16	19.10 ± 1.97
	30.3	11.33 ± 0.71	10.79 ± 0.68
	40.4	6.18 ± 0.31	6.09 ± 0.31
	45.5	5.38 ± 0.29	5.33 ± 0.29
	55.6	4.39 ± 0.22	4.37 ± 0.22
	70.7	4.67 ± 0.08	4.67 ± 0.08
	80.7	6.15 ± 0.13	6.15 ± 0.13
	85.7	6.79 ± 0.11	6.79 ± 0.11
	90.7	7.29 ± 0.09	7.29 ± 0.09
	100.7	8.82 ± 0.10	8.82 ± 0.10
	105.7	8.80 ± 0.18	8.80 ± 0.18
	110.7	8.82 ± 0.15	8.82 ± 0.15
	120.6	9.21 ± 0.16	9.21 ± 0.16
	130.5	8.26 ± 0.16	8.26 ± 0.16
	140.4	8.14 ± 0.16	8.14 ± 0.16
	150.4	6.77 ± 0.17	6.77 ± 0.17
	160.2	6.39 ± 0.17	6.39 ± 0.17
49.7	25.3	16.29 ± 0.91	15.80 ± 0.88
	30.4	13.48 ± 0.60	13.43 ± 0.60
	40.5	10.22 ± 0.44	10.20 ± 0.44
	45.5	7.76 ± 0.33	7.76 ± 0.33
	55.6	4.37 ± 0.08	4.37 ± 0.08
	60.6	3.97 ± 0.07	3.97 ± 0.07
	70.7	4.19 ± 0.07	4.19 ± 0.07
	80.7	5.88 ± 0.09	5.88 ± 0.09
	85.7	6.51 ± 0.09	6.51 ± 0.09
	90.7	7.17 ± 0.16	7.17 ± 0.16
	100.7	8.02 ± 0.17	8.02 ± 0.17
	105.7	7.84 ± 0.17	7.84 ± 0.17
	110.7	7.67 ± 0.12	7.67 ± 0.12
	120.6	6.65 ± 0.08	6.65 ± 0.08
	130.6	5.62 ± 0.09	5.62 ± 0.09
	140.5	4.71 ± 0.09	4.71 ± 0.09
	150.5	3.83 ± 0.07	3.83 ± 0.07
	160.3	3.29 ± 0.07	3.29 ± 0.07

[a] Cross section values do not include corrections for effects of multiple scattering, finite solid angle, and finite beam geometry. Uncertainties indicate only relative uncertainties from point to point. There is in addition a normalization uncertainty of 7% for each angular distribution.

[b] These are the same cross section values as in the previous column, except that corrections have been made for multiple scattering, finite solid angle, and finite beam geometry, as described in the text.

IV. ANALYSIS

Over the past few years, much theoretical work has been done to construct a high-order π-nucleus

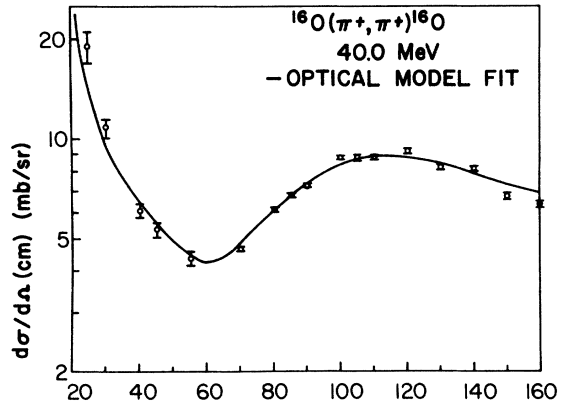

FIG. 2. Angular distribution at 40.0 MeV for the elastic scattering of positive pions on ^{16}O. The solid curves are first-order optical model fits to the data, as described in the text.

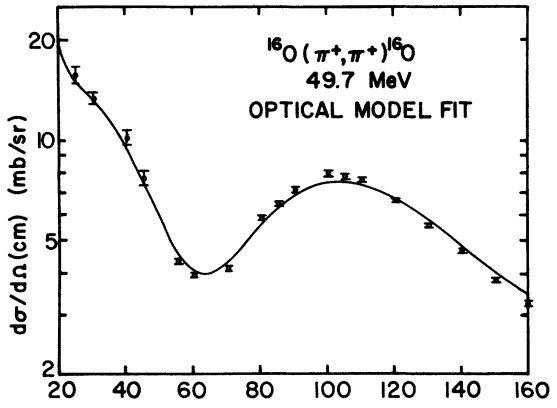

FIG. 3. Angular distribution at 49.7 MeV for the elastic scattering of positive pions on ^{16}O. The solid curves are first-order optical model fits, as described in the text.

optical potential. The predictions of such a potential will hopefully be compared with the present data. Here we have the more limited objectives of analyzing the data to give a representation in terms of π-nucleus partial waves, and in terms of a phenomenological first-order zero-range optical potential. Such phenomenological representations may eventually be useful in describing the data over wide ranges of incident energy and atomic weight. Such representations may also be useful in describing pion wave functions near the nucleus; however, the validity of such wave functions inside the nucleus needs to be examined. For the Kisslinger potential in particular, the wave function inside the nucleus can have sharp cusps. Such wave functions may be reasonable representations for low momentum transfer reactions such as inelastic pion scattering, although their validity for high momentum transfer reactions such as (p,π) is doubtful.

A. Partial wave representation of the data

We have analyzed the data using a partial-wave analysis code written by Gibbs, Gibson, and Stephenson.[20] In this code the scattering amplitude is written as

$$f(\theta)=f_c(\theta)+\frac{1}{2ik}\sum_{l=0}^{l_{\max}}(\eta_l e^{2i\delta_l}-1)e^{2i\sigma_l}(2l+1)\times P_l(\cos\theta), \quad (1)$$

where $f_c(\theta)$ is the complete Coulomb amplitude, $l_{\max}$ is the highest partial wave considered, η_l and δ_l represent the magnitude and phase of the elements of the nuclear scattering amplitude, and σ_l is the relativistic point charge Coulomb phase shift for the lth partial wave. We have fitted the 40.0 and 49.7 MeV data (column 4 of Table II) using $l_{\max}=2$ or $l_{\max}=3$. The good χ^2 unitary solutions (those in which all η_l's are ≤ 1) and solutions which are very close to being unitary are shown in Table III. Also shown in the table are the total

TABLE III. Low energy π^+-^{16}O elastic scattering phase shift parameters deduced from a partial-wave analysis.

Solution	T_π (MeV)	l	η_l	δ_l (deg)	χ^2 per degree of freedom	σ(total) (mb)
		0	1.02	−8.8		
A	49.7	1	0.64	13.0	1.3	334
		2	0.93	7.6		
		3	1.00	1.1		
		0	0.74	−18.2		
B	49.7	1	0.84	12.3	1.3	340
		2	0.91	7.8		
		3	0.98	0.9		
		0	0.97	−15.5		
C	40.0	1	0.90	8.2	2.5	228
		2	0.94	3.6		

cross sections as determined by the imaginary part of the forward scattering amplitude. The solutions for 49.7 MeV with $l_{max}=3$ have η_3 approximately unity and δ_3 approximately zero, indicating that there is very little nuclear scattering for $l \geq 3$. This is as expected for low-energy π-nucleus scattering. We consider the good fits which were obtained for reasonably small values of l_{max} to be an indication of the general consistency of the data. The normalizations of the angular distributions were varied and it was found that moving the normalization within the quoted uncertainties did not improve the partial wave fits.

For the 49.7 MeV data, two qualitatively different partial wave solutions were found. Solution A contains more absorption in the p wave than in the s wave and vice versa for solution B. The value for δ_0 is also significantly different for the two solutions. At 40.0 MeV, p-wave absorption is apparently stronger than s-wave absorption. If the phase shifts extracted from partial wave analyses such as these are to be taken seriously, then one would expect the phase shifts to vary smoothly with nuclear size and with energy. Thus, this kind of analysis, carried out for many energies and targets, may determine unambiguous phase shifts.

B. Optical model analysis

The elastic scattering data (column 4 of Table II) were compared with optical model calculations carried out with the FITPI code of Cooper and Eisenstein.[21] We used this code to solve a modified Klein-Gordon equation with a Kisslinger-model potential

$$U(r) = -b_0 k^2 \rho(r) + b_1 \vec{\nabla} \cdot \rho(r) \vec{\nabla}, \quad (2)$$

where $\rho(r)$ is the nuclear density, k is the incident pion wave number, and b_0 and b_1 are complex parameters related to the pion-nucleon amplitudes. We use the notation b_{0R} and b_{0I} for the real and imaginary parts of b_0, and similarly for b_1. A modified Gaussian density function

$$\rho(r) = \frac{K^3}{3(\sqrt{\pi}R)^3}\left[1+2\left(\frac{Kr}{R}\right)^2\right]\exp\left(\frac{-K^2r^2}{R^2}\right) \quad (3)$$

was used for both the nuclear potential and charge densities, where R is the appropriate rms radius and $K=1.5$ for ^{16}O.[22] The charge distribution in ^{16}O as determined by electron scattering has an rms radius of 2.71 fm. The value of R which was used for the charge density was 2.80 fm, corresponding to adding the pion charge radius of 0.71 fm in quadrature to the rms radius of the proton distribution. Similarly, the value of R which was used for the nuclear potential was 2.59 fm, corresponding to subtracting the proton charge radius of 0.80 fm. This was done to be consistent with the model assumption of zero-range pion-nucleon interactions.

With the densities fixed, we varied the potential parameters b_0 and b_1, and determined separately the best fit values at 40.0 and 49.7 MeV. The optical model fits are shown in Figs. 2 and 3 along with the data. The b_0 and b_1 values are given in Table IV. The χ^2 per degree of freedom are also given for each fit. Uncertainties for the best fit b_0 and b_1 values are typically about 0.2 fm^3. We also show in Table IV the b_0 and b_1 values we deduced from a reanalysis of previous π^+-^{16}O data at $T_\pi = 30$ MeV subject to the constraint that the solution be unitary. These values are slightly different from those published previously. For the 30 MeV data nonunitary solutions with a slightly lower χ^2 were also found, but these were discarded because they are unphysical. The low χ^2 for the 30.0 MeV data may merely reflect the fact that the uncertainties in that data are much larger than for the present data at 40.0 and 49.7 MeV. The energy dependence found here for the Kisslinger model optical parameters b_0 and b_1 is in good agreement with that given by Auerbach, Fleming, and Sternheim[23] in an analysis of earlier data.

It is important to be cautious in interpreting the values we have found for b_0 and b_1. Fitting the data with a potential that includes higher-order effects would certainly change the values deduced

TABLE IV. Best fit values for the Kisslinger-potential parameters b_0 and b_1, and for σ(total), σ(reaction), and σ(elastic) for low-energy π^+-^{16}O elastic scattering.

T_π (MeV)	b_{0R} (fm^3)	b_{0I} (fm^3)	b_{1R} (fm^3)	b_{1I} (fm^3)	χ^2 per degree of freedom	σ(total) (mb)	σ(elastic) (mb)	σ(reaction) (mb)
49.7	−3.12	0.01	6.21	0.84	5.5	284	100	184
40.0	−3.64	0.10	6.27	0.79	5.2	230	89	141
30.0	−4.56	0.38	5.47	0.17	2.5	108	64	44

for b_0 and b_1. The partial-wave fits described above probably represent the best χ^2 fits to the angular distributions that can be obtained. It is not surprising, therefore, that χ^2 per degree of freedom values of ~5 are obtained for the optical model fits, where the model is more restrictive. It is to be expected that more sophisticated optical model calculations will be able to fit the data with lower values of χ^2; for example, one might take into account a finite range in the pion-nucleon interactions, pion absorption, etc. It is important to note in this connection that the quality of the optical model fit is very sensitive to the potential radius value R. Increasing R from 2.59 fm to about 2.67 fm (for example, to simulate finite range effects) significantly improves the phenomenological fits (giving $\chi^2 = 1.2$ at 49.7 MeV and $\chi^2 = 3.7$ at 40.0 MeV), also with large changes in the resulting best fit values of b_0 and b_1. However, we have chosen not to consider R a phenomenological parameter, since we expect effects such as finite range to eventually be treated explicitly.

In Table IV we show also the values for σ_{total}, σ_{reaction}, and σ_{elastic} calculated from the best fit optical potential parameters. Uncertainties are not shown, but are related to the overall normalization uncertainties in the data, and to the model uncertainties in extrapolating to forward and backward angles. The total cross sections from the optical model and phase-shift analyses are in reasonable agreement, with the biggest difference being 17% at 49.7 MeV. It will be of interest to compare these values with those deduced by other techniques.

For the FITPI code the scattering amplitude can be written

$$f(\theta) = f_c(\theta) = \frac{1}{2ik} \sum_{l=0}^{l_{\max}} (\eta_l e^{2i\delta_l} - 1) S_{Cl} (2l+1) P_l(\cos\theta) , \tag{4}$$

where parameters are similar to those defined for Eq. (1) above. S_{Cl} gives the relativistic Coulomb effects for a finite size nucleus. Table V shows the η_l and δ_l values for $l \leq 3$ obtained for the optical potential solutions. For $l > 3$ there is essentially no nuclear effect on the scattering.

TABLE V. Phase shift parameters for low-energy π^+-^{16}O elastic scattering deduced from best fit Kisslinger potential.

T_π (MeV)	l	η_l	δ_l (deg)
49.7	0	0.84	−18.6
	1	0.78	13.0
	2	0.92	6.9
	3	0.99	1.1
40.0	0	0.93	−18.6
	1	0.85	10.5
	2	0.96	4.2
	3	1.00	0.5
30.0[a]	0	0.95	−17.3
	1	0.97	5.6
	2	1.00	1.7

[a] Data from Ref. 7.

It is interesting to note that the phase shifts shown in Table V have much the same character as all the partial-wave solutions shown in Table III except for solution A.

V. CONCLUSIONS

We have presented angular distributions for elastic scattering of π^+ on ^{16}O at 40.0 and 49.7 MeV. The data were analyzed in terms of π-nucleus partial waves and phenomenological parameters of a first-order Kisslinger optical model potential. Good fits were obtained with scattering amplitudes which preserve unitarity.

ACKNOWLEDGMENTS

The authors would like to thank the members of the staff of LAMPF for their help and encouragement during the running of this experiment. We extend special thanks to N. Hill of ORNL for his assistance in the design of electronics components necessary for the high-efficiency operation of the π-μ systems. We also thank W. R. Gibbs, B. F. Gibson, and G. J. Stephenson, Jr. for providing us with their partial-wave analysis code and for many helpful discussions.

†On leave from Tel Aviv University, Ramat Aviv, Israel.

*Supported in part by the Office of Naval Research and by the National Science Foundation
‡Supported by the USERDA.
§Operated by Union Carbide Corporation, under contract with the USERDA.
¶Supported by the National Science Foundation.

[1]See, for example, review articles by D. S. Koltun, Adv. Nucl. Phys. 3, 71 (1969); M. M. Sternheim and R. R. Silbar, Annu. Rev. Nucl. Sci. 24, 249 (1974).
[2]M. M. Sternheim and E. H. Auerbach, Phys. Rev. Lett. 25, 1500 (1970).
[3]M. Blecher, K. Gotow, D. K. Anderson, R. Kerns, R. Minehart, K. Ziock, R. W. Bercaw, J. S. Vincent, and R. Johnson, Phys. Rev. C 10, 2247 (1974).
[4]M. Thies, Phys. Lett. 63B, 39 (1976).
[5]M. Krell and S. Barmo, Nucl. Phys. B20, 461 (1970).

[6]K. M. Crowe, A. Fainberg, J. Miller, and A. S. L. Parsons, Phys. Rev. 180, 1349 (1969).
[7]J. F. Marshall, M. E. Nordberg, Jr., and R. L. Burman, Phys. Rev. C 1, 1685 (1970).
[8]J. F. Amann, P. D. Barnes, M. Doss, S. A. Dytman, R. A. Eisenstein, and A. C. Thompson, Phys. Rev. Lett. 35, 426 (1975).
[9]H. Dollard, K. L. Erdman, R. R. Johnson, H. R. Johnston, T. Masterson, and P. Walden, Phys. Lett. 63B, 416 (1976).
[10]S. A. Dytman, J. F. Amann, P. D. Barnes, J. N. Craig, K. G. R. Doss, R. A. Eisenstein, J. D. Sherman, W. R. Wharton, R. J. Peterson, G. R. Burleson, S. L. Verbeck, and H. A. Thiessen, Phys. Rev. Lett. 38, 1059 (1977).
[11]D. Malbrough, R. D. Edge, C. W. Darden, T. Marks, B. M. Preedom, F. Bertrand, E. E. Gross, C. A. Ludemann, M. J. Saltmarsh, R. L. Burman, R. P. Redwine, K. Gotow, and M. A. Moinester, Bull. Am. Phys. Soc. 21, 983 (1976).
[12]R. L. Burman, R. L. Fulton, and M. Jakobson, Nucl. Instrum. Methods 131, 29 (1975).
[13]P. A. M. Gram (private communication).
[14]M. J. Saltmarsh, B. M. Preedom, R. D. Edge, and C. W. Darden, III, Nucl. Instrum. Methods 105, 311 (1972); and N. Hill, M. A. Moinester, F. Bertrand, D. Malbrough, and K. Gotow (unpublished).
[15]P. Y. Bertin, B. Coupat, A. Hivernat, D. B. Isabell, J. Duclos, A. Gerard, J. Miller, J. Morgenstern, J. Picard, P. Vernin, and R. Powers, Nucl. Phys. B106, 341 (1976).
[16]D. Axen, G. Duesdieker, L. Felawka, C. H. Q. Ingram, G. Jones, M. Salomon, and W. Westlund, Nucl. Instrum. Methods 118, 435 (1974).
[17]B. M. Preedom (unpublished).
[18]D. C. Dodder (private communication).
[19]J. L. Friar and J. W. Negele, *Advances in Nuclear Physics*, edited by M. Baranger and E. Vogt (Plenum New York, 1975), Vol. 8.
[20]W. R. Gibbs, B. F. Gibson, and G. J. Stephenson, Jr., Los Alamos Scientific Laboratory Report No. LA-UR-77-1404 (unpublished).
[21]M. D. Cooper and R. A. Eisenstein, Los Alamos Scientific Laboratory Report No. LA-5929-MS, 1975 (unpublished).
[22]H. R. Collard, L. R. B. Elton, R. Hofstadter, and A. Schopper; *Landolt-Börnstein Numerical Data and Functional Relationships in Science and Technology*, edited by K. H. Hellwege (Springer-Verlag, Berlin, 1967), New Series, Group 1, Vol. 2.
[23]E. H. Auerbach, D. M. Fleming, and M. M. Sternheim, Phys. Rev. 162, 1683 (1967).